Az „ón pestis” jelenségének kutatása villamos mérések segítségével

Kutatási jelentés

I. 1 INTRODUCTION

Tin (Sn) is one of the most important materials in the electronics technology, this is the base metal in most of the solder alloys and is used as surface finishing of the solder pads and components leads. Sn has four allotropes: α, ß , γ and σ Sn. From these, ß-Sn (white Sn) is the metallic form and it is applied in the electronics technology. ß-Sn is stable between 13.2 and 231.9°C, it has *bct* (body-centered tetragonal) structure crystallizing in the space-group symmetry $I4_1/amd$ (No. 141) with lattice parameters a = 5.8316 Å and c = 3.1815 Å. The α-Sn (gray Sn) is a non-metallic form, which is stable below 13.2°C, it has diamond structure with cubic symmetry *Fd3m* (No. 227), lattice parameter a = 6.4892Å. α-Sn is brittle and has semiconductor properties. The other two allotropes, γ and σ, exist only at very harsh circumstances, over 161 °C and in high pressure [1]. For ß →α transition the relative stability of the system is defined by its Gibbs free energy G=H-TS, where H - enthalpy, T- temperature and S - entropy. The system is in thermodynamic equilibrium when the Gibbs free energy reaches a minimum. This is associated with the progress of the system to the state with the lowest internal energy U and the highest entropy S.

Tin pest is a spontaneous allotropic transition of ß-Sn to α-Sn below 13.2°C. In basic case the transition is slow to initiate due to a high activation energy but the presence of materials with the same crystal structure and close lattice parameters to the α-Sn or very low temperatures (under −30°C) can speed up the process considerably. The transition causes also a large volume increase of about 27% [2]. The α-Sn transition is a process of nucleation and growth [3]. Nucleation is the first step in the formation of either a new thermodynamic phase or a new structure via self-organization. Firstly, a new phase (α-Sn) appears at certain sites within the metastable parent phase (ß-Sn). Homogeneous nucleation occurs spontaneously and randomly without preferred nucleation sites, while heterogeneous nucleation occurs at especially vulnerable sites, such as grain boundaries, dislocations or impurities. The signs of the transition starts from blemishes, discoloration, mottling. Later these first ones are changed into characteristic warts, which originates the name “tin pest”.

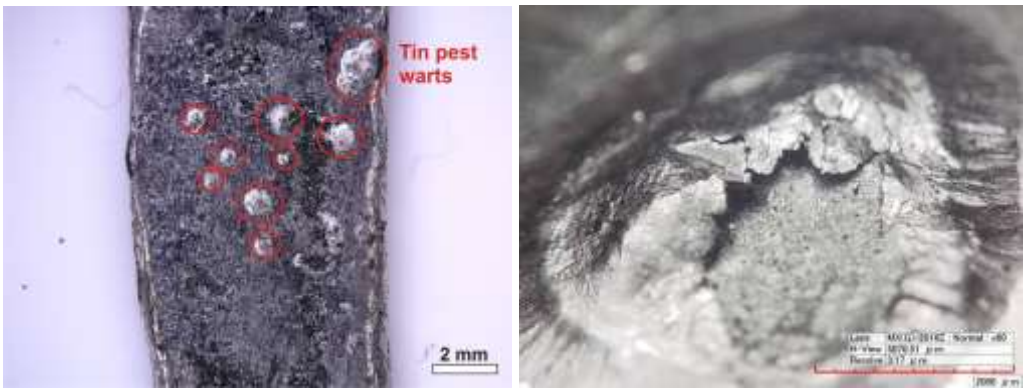

Fig. 1. ß→α transition: a) α-Sn warts on the surface of Sn object; b) blistering of α-Sn.

Finally the sample is changed into the form of the powder leading to the total disintegration of the Sn sample which is related to the volume increase and the very low ductility of the Sn resulting in material blistering and cracking (Fig. 1) [4]. The tin pest is an autocatalytic reaction, which means that the appearance of α-Sn speeds up the transition leading to sample disintegration. The identification and characterization of tin pest in Sn-rich solders and surface finishes is crucial for electronic devices working in sub-zero temperatures in aeronautical, aerospace and automobile applications [5].

The α-Sn transition can be avoided by alloying with small amount of electropositive metals which are soluble in solid phase of Sn, such as antimony or bismuth. In the past, another effective method was the application of high Pb content alloys, since Pb blocks the α-Sn transition effectively similar to the case of tin whisker growth [6]. Therefore, before the RoHS (Restriction of Hazardous Substances) directives of the European Commission, the tin pest phenomenon was less frequent in electronics appliances. However since 2006, electronic manufacturers must replace the SnPb solder alloys with high Sn content (<90%) lead-free solder alloys, which means a real risk of a Sn allotropic transition in solder joints as well as in surface finishes and coatings [7]. Nevertheless, the literature is not straight forward in the behavior of high Sn content alloys. There are some studies which stated that the tin pest is impossible in binary and trinary Sn alloys [8, 9], but there are researches where the phenomenon occurred in high Sn content alloys as well [2, 5]. The presence of elements soluble in Sn - Pb, Bi, Sb suppresses the transition by raising the transition temperature and that Cd, Au and Ag rephrase it [10]. Insoluble elements, such as Zn, Al, Mg and Mn accelerate the transition by lowering the temperature at which it occurs while Cu, Fe and Ni are reported to have little influence [11, 12]. The tin pest phenomenon is difficult to study in natural conditions since the nucleation phase is very slow, so the first signs of transition are noticeable only after several months [3].

Application of the seeds or inoculators – such as CdTe or InSb or α-Sn itself [4] – could speed up the nucleation phase considerably. By introducing the CdTe or InSb surface inoculators, heterogeneous nucleation is initiating. Heterogeneous nucleation with the nucleus at a surface, is much faster than homogeneous nucleation because the nucleation barrier ΔG^* is much lower at a surface. This is because the nucleation barrier comes from the positive term in the free energy ΔG, which is the surface term. It is at the stage the atoms arrange in a defined and periodic manner that defines the crystal structure. Later, the further growth is the subsequent size increase of the nuclei that succeed in achieving the critical size, in case of ß→α-Sn transition, based on coherent, diffusion less displacements of large number of atoms.

These inoculation techniques, however, are not accurate enough to predict nucleation time in real working conditions or to simulate real-life situations, since the acceleration factor of these inoculators are not known. Still they are very useful to study the nature of the process and the growth of the α phase, as it is possible to compare different Sn alloys under same conditions, which can provide useful information about the nucleation times for different alloys [13]. In addition CdTe and InSb are widely used in electronics. InSb which has a small direct bandgap (0.17 eV) and the highest electron mobility (77000 cm^2/Vs) among all known semiconductors, is an attractive material for high-speed electronics and infrared optoelectronics [14]. It is also popular material used for MOSFET transistors and to produce different electronic substrates [15]. CdTe is an alternative material for photovoltaic solar cells [16, 17]. Therefore both of these substances can have a “meet” with Sn-based solder joints.

The α-Sn transition can be investigated by imaging methods such as optical microscopy [4], Scanning Electron Microscopy (SEM) [18] and Focused Ion Beam – Scanning Ionic Microscopy (FIB-SIM), since the transition has visual traces on the surface as well as in the

inside of the samples. The amount of the transitioned α-Sn can be measured among the others by X-Ray diffraction (XRD) [19] and Mössbauer spectroscopy [20]. The phenomenon can be characterized by electrical resistance measurements [21], since there is the change from metal to semiconductor leading to the electrical resistance value change.

The aim of this work was to characterize α-Sn allotropic transition in SnCu1 bulk alloy inoculated by InSb with the electrical resistance measurements and to analyse the characteristics by optical microscopy and by FIB-SIM at the cross-sections to gain more knowledge about ß→α transition.

II. MATERIALS AND METHODS

The samples were prepared with the tin pest induction method developed earlier [13]. For the investigation, samples were prepared using mechanical treatment (cold-rolling and axial compression) on SnCu1 bulk alloy (purity of 99.9 wt. %) with two different sizes: S1: 45x6x1.5mm3 and S2: 45x6x3mm^3 size. The SnCu1 alloy is widely used for wave and selective selective soldering, and the 1% Cu alloying makes the solder very prone to tin pest [5]. The average electrical resistance value of the samples was 0.5mΩ and 0.25 mΩ for S1 and S2, respectively. The electrical resistance deviation was 4%, due to the deviation of the sample size. All together 15-15 sample pieces were inoculated by InSb inoculator powder, which was pressed into the upper layer of the samples by a mechanic laminator with 30kN force (Fig. 2). Before inoculation, the samples were dipped in a HCl solution to remove the oxide layer which may prevent the transformation The samples were stored at -18 °C for 42 days (6 weeks) in a refrigerator.

The transition progress was monitored by 4-probe electrical resistance measurement of the samples with an AGILENT 4338B milliohm meter at room temperature. The measurement accuracy of the instrument at the mΩ range was under 3%. The repeatability error of the resistance measurements was under 2%.

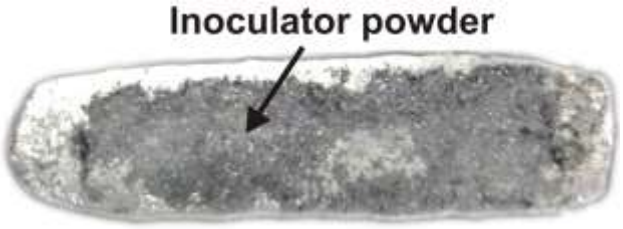

Fig. 2. Inoculated sample before the test.

During the tests, cross-sections were also prepared from the samples to compare the resistance changes with the amounts of transformed Sn in the samples. From given samples ten cross-sections were prepared to get more information about the uneven development of α-Sn. The developed α-Sn warts were also etched with FIB (focused ion beam, JEM-9320-FIB) and were observed by FIB-SIM with a 60° tilt angle (with a Ga ion source and acc. voltage of 30 kV) in order to study the layer structure of tin pest wards and to identify the different allotropes.

III. RESULTS

Fig. 3 and Fig. 4 show the electrical resistance increases on a logarithmic scale in the function of time. During the first 7 days, no detectable resistance change was observed. At both sample types, some resistance increases were found after the 2 weeks, but the highest

increase was under 6% which value is very close to the repeatability and measurement error. However, the warts typical for α-Sn already appeared on the surface of certain samples (Fig. 1). After 3 weeks of storage at -18 °C, all of the samples showed an increase in resistance between 5 and 20%, therefore the nucleation phase of the α-Sn development in this study was determined to be 3 weeks.

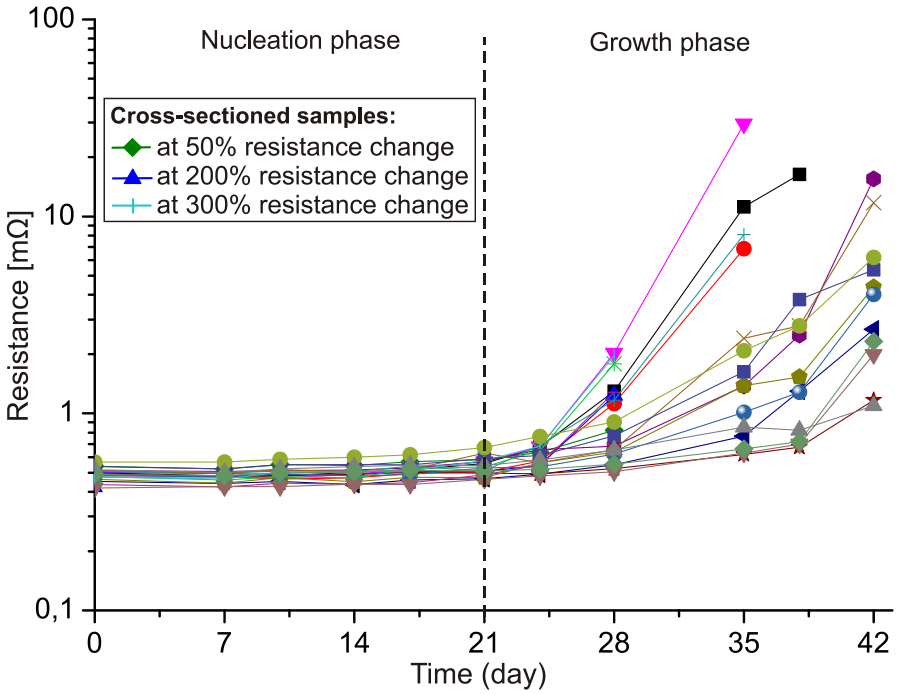

Fig. 3. Electrical resistance increase of S1 samples during the test.

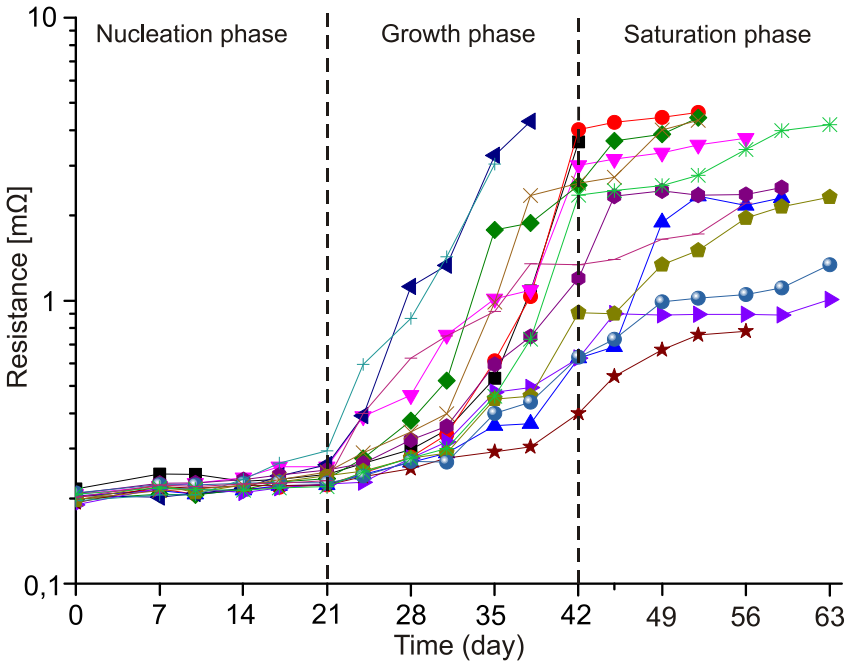

Fig. 4. Electrical resistance increase of S2 samples during the test.

After 3 weeks, when the nucleation phase has been over, the increase of electrical resistance was considerable. However, the deviation of the resistance increase was also very high. After 4 weeks of storage at -18 °C, the resistance) changes were between 1.1 and 3

times, and after 5 weeks they were between 1.25 and 20 times. This effect was caused partially by uneven inoculation of the samples, but much more by the stochastic development nature of the α-Sn transition. Since the process is highly autocatalytic, only a small difference in time or in α-Sn results in big differences in transition rate of the different samples. This is clearly visible in Fig. 3 and 4, as the deviation is increasing with time in the nucleation phase.

In the case of the S1 samples, it was observed after 5 weeks of storage at -18 °C that some of the S1 samples decomposed by the α-Sn transition into powder and bigger sized morsels. This effect is presented in Fig. 5. The disintegration of the S1 samples usually occurs when the electrical resistance of the samples increase by 25 – 30 times. The highest measurable resistance changes for S1 samples was 32 times after 5 weeks of storage at -18 °C. In this case the tests had to be finished after 6 weeks, since most of the samples have been decomposed.

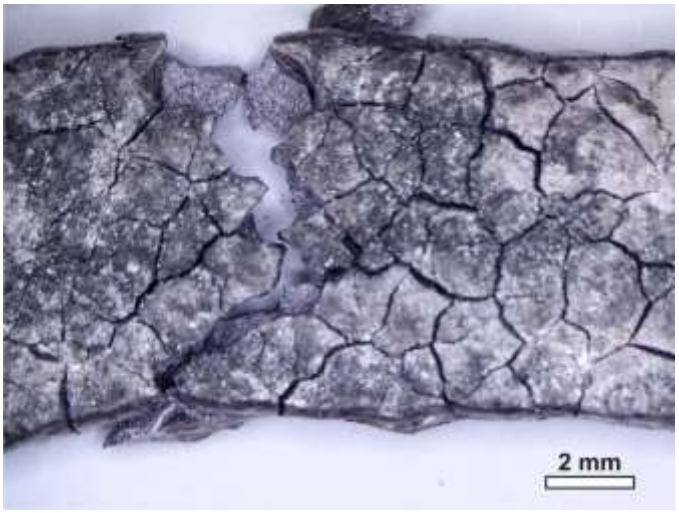

Fig. 5. Disintegrated S1 sample by α-Sn transition after 6 weeks of storage at -18 °C.

In the case of S2 samples, the larger thickness ensured longer testability; these samples had higher mechanical stability than the S1 samples. Interestingly, the electrical resistance increase reached a "saturation state" after 6 weeks (Fig. 5), the resistances barely changed between the 6th and 9th week. After 8-9 weeks of storage at -18°C these samples started to decompose as well and the test had to be stopped. The highest measurable resistance changes for the S2 samples was 65 times after 8 weeks of storage at -18 °C.

After 3 weeks of storage at -18 °C, three S1 samples with 50% and 200% resistance increase, were selected and pulled out for the test to examine its cross-sections, in order to compare the amount of transitioned Sn with the measured resistance increase (Fig. 6). (Samples with higher resistance changes were not suitable for cross-sectioning since they became very brittle.) Cracks were found in the cross-sections, however these are not real cracks but holes from where the transformed α-Sn is missing. As it was discussed earlier, the mechanical strength of α-Sn is much worse than the mechanical strength of ß-Sn. Therefore these holes were formed during the gridding of the samples (as a necessary step of the cross-section preparation), when the emerging α-Sn usually fell out from the sample body. The holes always begin from the surface of the sample which is also a clear evidence that they are created by the transition. With cross-sectioning only the 2D projections of the 3D holes can be studied, thereby no correlation was found between the sizes and amounts of the holes.

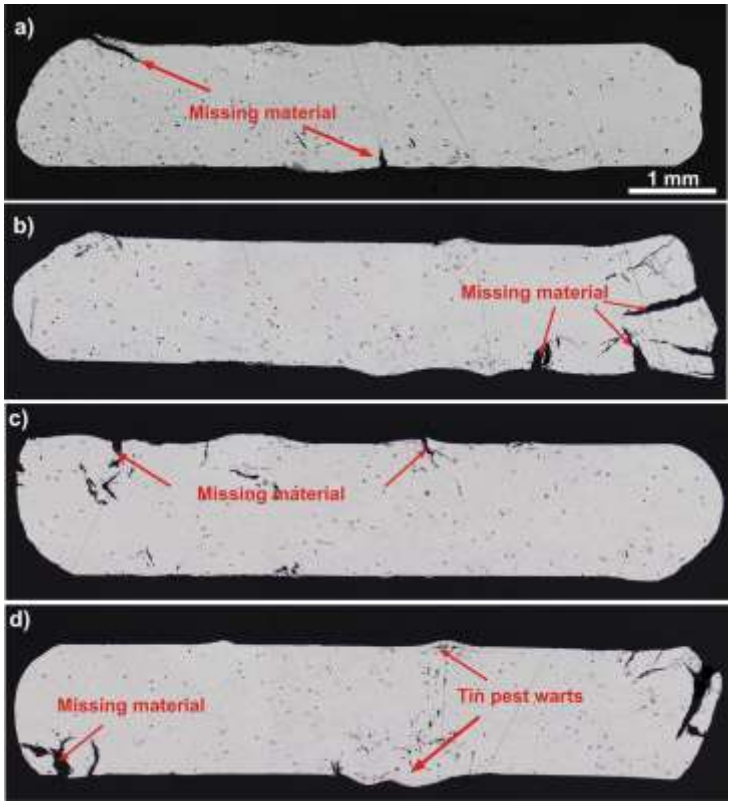

Fig. 6. Cross-sections of an S1 sample, a-b: after 50% of resistance increase; c-d: after 200% of resistance increase.

A typical tin pest wart related to the volume change during the transition, is well observable in Fig. 6d), at these areas the tin pest penetrated some tens of μm into the surface. Rearrangement of the Sn atoms, leading to bigger crystal unit (cubic) formation, causes volume expansion resulting in blistering of the material.

VI DISCUSSION

The electrical resistance measurement has proven to be a good characterization method for ß→α transition. The sensitivity of the method is high, already a 10% resistance change is surely detectable. Di Maio and Hunt studied the electrical resistance changes of different Sn alloys (Sn, SnCu, SnAg, SnNi, SnZn, SnIn and SnPb) inoculated with CdTe at -35 °C [21]. They also observed a relatively long nucleation phase which is followed by a fast growth of α-Sn phase where the electrical resistance increased considerably (in their case, the speed of the transition was much higher due to the lower storage temperature). However, they reached the saturation phase only at rare solder alloys like SnIn and SnNi.

It was found that that the ß→α transition significantly slows down after the rapid growth phase and the process is saturated. Similar results were observed in our previous research by Mössbauer spectroscopy [20]. Detailed data analysis with respect to local symmetries of Sn nuclei reveals two signals deriving from α-Sn and ß-Sn phases, as one can be seen in Fig. 7. The ratio of both Sn phases was found near equal which was an intriguing result considering that the investigated sample was a grey fine powder of Sn (tin pest) after 6 years of exposure at -18°C [20].

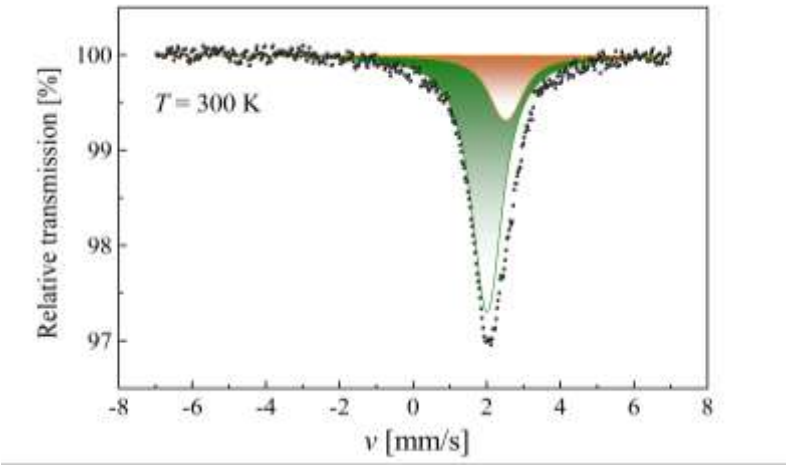

Fig 7. Mössbauer spectrum (A) of grey Sn powder (B). The more intense line located at 2 mm/s corresponds to α-Sn phase (green line), while the second line indicates the parent ß-Sn phase (orange line).

Therefore, it is assumed that above a certain contribution of α-Sn into the overall volume of small Sn pieces, the ß to α-Sn transition is stopped. To prove above the hypothesis further analysis were done by FIB-SIM.

During the preparation of the FIB cross-sections, non-transitioned ß-Sn grains were found even on the surface of the samples. Fig. 8 shows an example where the transition occurred around a single crystalline ß-Sn grain, but the grain itself remained non-transitioned, no traces of α-Sn or subgrain development can be seen on its cross-section. The transitioned α-Sn is already missing around the non-transitioned ß-Sn grain, leaving a hole after itself.

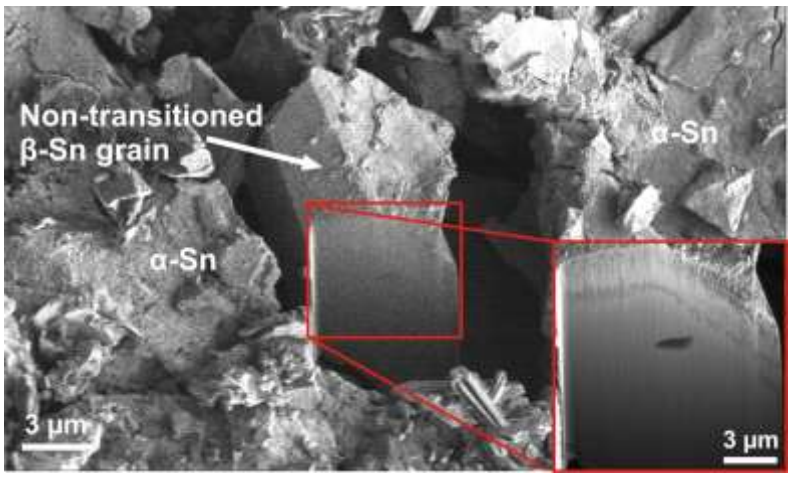

Fig. 8. Non-transitioned ß-Sn grain at the surface of the sample.

Fig. 9 shows a FIB cross-section made at a transitioned area of the sample. The border of the transition can be determined clearly according to the sizes and contrast difference between the ß and α-Sn grains. The FIB-SIM examination confirmed the results of the Mössbauer measurement that not all of the ß-Sn transitioned, since even the hypothetically completely transitioned areas contain non-transitioned ß-Sn grains (Fig. 9).

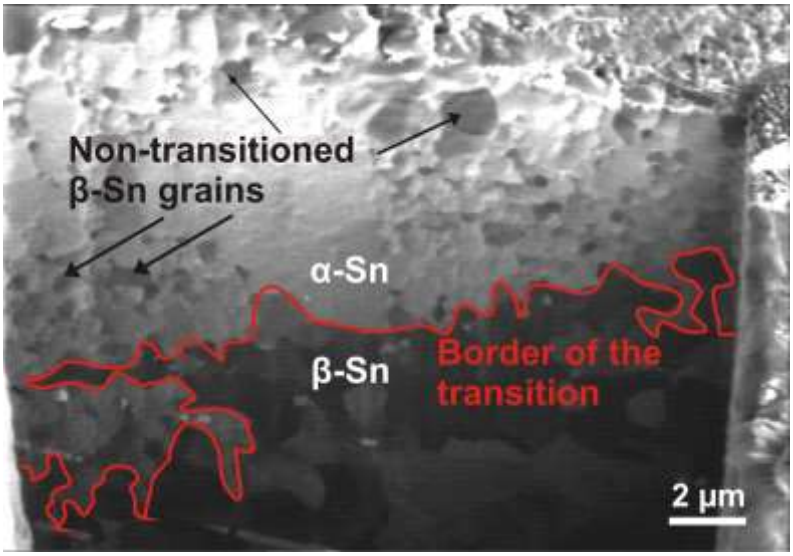

Fig. 9. FIB-SIM micrograph on ß to α-Sn transition inside the sample body.

According to our results, the development of α-Sn starts at the surface of the sample and after some time the tin pest penetrates inside the sample causing the decomposition of the sample to smaller pieces. However, the newly developed α-Sn can enclose non-transitioned ß-Sn inhibiting its further transition. In this case, ß-Sn remains still present in the middle of the sample entrapped by α-Sn, although it is in the metastable state. The reason of the remaining of non-transition of ß-Sn might be the following: where α-Sn encloses metastable ß-Sn, the considerable volume increase (27%) causes local mechanical stress and local change of the pressure. The Gibbs free energy (G) value, guarantying the thermodynamic equilibrium of two phases (α and ß-Sn) is strongly influenced by pressure value. If the value of the pressure is changed, even locally, the thermodynamic equilibrium is shifted.

During the optical investigations (Fig. 6) it was observed that in this case the development of tin pest progress differs from typical observations, where the α-Sn develops faster horizontally than vertically in the sample body. That kind of development results in the forming of "disc like" layer separations, one by one towards the middle of the sample body [4, 5]. In this study, evidence was found that the vertical expansion of the α-Sn can be the same or sometimes even faster than the horizontal expansion. Fig 10 shows a FIB-SIM micrograph where it is visible how the α-Sn expands vertical direction from grain to grain.

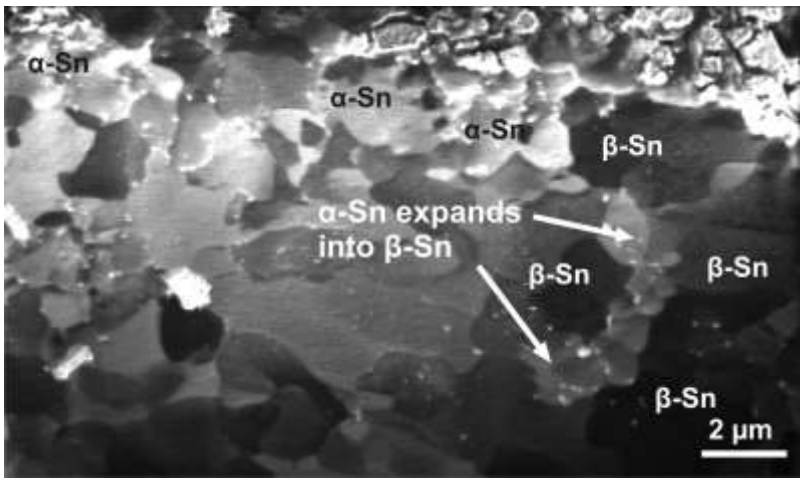

Fig. 10. FIB-SIM micrograph showing vertical expansion of α-Sn into ß-Sn grains.

This is partially visible in Fig. 9 as well. This effect could be the result of the InSb inoculator, since the typical observations of α-Sn expansion were found in non-inoculated samples or with an α-Sn inoculator [4, 5]. However it is also likely that the proneness for the α-Sn transition depends on the grain orientation. Further research is necessary to prove these hypotheses.

V. CONCLUSIONS

The α-Sn transition was characterized by electrical resistance measurements. The electrical resistance measurement has proven to be a good characterization method for tin pest phenomenon. The sensitivity of the method is high, resistance change of 10% is already detectable. In the case of SnCu1 solder alloy, the α-Sn transition has three stages: nucleation, growth and saturation phase. At the saturation phase the transition is almost stopped. It was shown by focused ion beam cross-sectioning and by Mössbauer spectroscopy results that the developed α-Sn can encloses the non-transitioned transformed ß-Sn inhibiting its further transition. The volume increase of transition may cause that the transition is stopped because of arising mechanical strain disturbing the atoms displacements and changed local pressure influencing the thermodynamical equilibrium. In our study the development of tin pest differed from typical observations when α-Sn expends faster horizontally than vertically in the sample body. Evidences were found that the vertical expansion of the α-Sn into the sample body can be the same or faster than the horizontally. This effect could be the results of the InSb inoculator and/or the different tin pest susceptibility of the ß-Sn grains with different orientations. However further researches are necessary to prove these assumption.

References

[1] A. M. Molodets, S. S. Nabatov, Thermodynamic Potentials, Diagram of State, and Phase Transitions of Tin on Shock Compression, High Temp. 38/5 (2000) 715–721.

[2] S. Gialanella, F. Deflorian, F. Girardi, I. Lonardelli, S. Rossi, Kinetics and microstructural aspects of the allotropic transition in tin, J. Alloys Compds 474 (2009) 134–139.

[3] W. Plumbridge, Recent Observations on Tin Pest Formation in Solder Alloys, J. Electron. Mater.37/2 (2008) 218–223.

[4] A. Skwarek, P. Zachariasz, J. Kulawik, K. Witek, Inoculator dependent induced growth of α-Sn, Mater. Chem. Phys. 166 (2015) 16-19.

[5] A. Skwarek, M. Sroda, M. Pluska, A. Czerwinski, J. Ratajczak, K. Witek, Occurrence of tin pest on the surface of tin-rich lead-free alloys, Solder. Surf. Mount Tech. 23/3 (2011) 184-190.

[6] B. Illés, B. Horváth, Whiskering Behaviour of Immersion Tin Surface Coating, Microelectron. Reliab. 53 (2013) 755-760.

[7] D. Di Maio, C. Hunt, On the absence of the ß to α Sn allotropic transformation in solder joints made from paste and metal powder, Microelectron. Eng. 88 (2011) 117–120.

[8] O. Semenova, H. Flandorfer, H. Ipser, On the non-occurrence of tin pest in tin–silver–indium solders, Scripta Mater. 52 (2005) 89–92.

[9] W. Peng, An investigation of Sn pest in pure Sn and Sn-based solders, Microelectron. Reliab. 49 (2009) 86–91.

[10] D. Giuranno, S. Delsante, G. Borzone, R. Novakovic, Effects of Sb addition on the properties of Sn-Ag-Cu/(Cu, Ni) solder systems, J. Alloys Compds 689 (2016) 918-930.

[11] W.J. Plumbridge, Tin pest issues in lead-free electronic solders, J. Mater. Sci. – Mater. Electron. 18 (2007) 307-318.

[12] M. Leodolter-Dworak, I. Stefan, W.J. Plumbridge, H. Ipser, Tin Pest in Sn-0.5Cu Lead-Free Solder Alloys: A Chemical Analysis of Trace Elements, J. Electron. Mater. 39/1 (2010) 105-108.
[13] A. Skwarek, J. Kulawik, K. Witek, Method of Evaluating the Susceptibility of Tin Alloys to Tin Pest, 2013 polish patent application number: P404330, patent number: 221478, filing date: 14.06.2013
[14] K. Zhang, Y. Wang, W. Jin, X. Fang, Y. Wan, Y. Zhang, L. Dai, High-quality InSb nanocrystals: synthesis and application in graphene-based near-infrared photodetectors, RSC Adv. 6/30 (2016) 25123-25127.
[15] T. Ito, A. Kadoda, K. Nakayama, Y. Yasui, M. Mori, K. Maezawa, T. Mizutani, Effective mobility enhancement in Al2O3/InSb/Si quantum well metal oxide semiconductor field effect transistors for thin InSb channel layers, Jpn. J. App. Phys. 52/4S (2013) 04CF01.
[16] A.Y. Shenouda, M.M. Rashad, L. Chow, Synthesis, characterization and performance of Cd 1− xInxTe compound for solar cell applications, J. Alloys Compds 563 (2013) 39-43.
[17] S.A. Vanalakar, G.L. Agawane, S.W. Shin, M.P. Suryawanshi, K.V. Gurav, K.S. Jeon, J.H. Kim, A review on pulsed laser deposited CZTS thin films for solar cell applications, J. Alloys Compds 619 (2015) 109-121.
[18] N. D. Burns, A Tin Pest Failure, J. Fail. Anal. Prev. 9/5 (2009) 461–465.
[19] K. Nogita, C.M. Gourlay, S.D. McDonald, S. Suenaga, J. Read, G. Zeng, Q.F. Gud, XRD study of the kinetics of β↔α transformations in tin, Philos. Mag. 93/27 (2013) 3627-3647.
[20] A. Skwarek, P. Zachariasz, J. Zukrowski, B. Synkiewicz, K. Witek, Early stage detection of ß to α a transition in Sn by Mössbauer spectroscopy, Mater. Chem. Phys. 182 (2016) 10-14.
[21] D. Di Maio, C.P. Hunt, Monitoring the Growth of the a Phase in Tin Alloys by Electrical Resistance Measurements, J. Electron. Mater. 38/9 (2009) 1874 – 1880.

A fent közölt kutatási eredmények publikálásra kerültek:
A. Skwarek, B. Illés, B. Horváth, A. Géczy, P Zachariasz, D. Bušek, Identification and caracterization of ß→α-Sn transition in SnCu1 bulk alloy inoculated with InSb, JOURNAL OF MATERIALS SCIENCE: MATERIALS IN ELECTRONICS 28 (2017) 16329–16335.

Készítette: Dr. Illés Balázs

Budapest, 2018.01.31.